International Journal of Science and Research (IJSR)
ISSN: 2319-7064
Impact Factor 2024: 7.101

Biomechanical Analysis of a Modified Proximal Femoral Nail in the Management of Reverse Obliquity Intertrochanteric Fractures: A Finite Element Study from East India

Dr. Bighnesh Dash[1], Dr. Hatia Marandi[2]

[2]Corresponding Author

Abstract: ***Background: Reverse obliquity intertrochanteric fractures (ROIFs) remain one of the most challenging proximal femoral fractures to stabilize, and the ideal fixation method continues to be debated. To address this, a modified proximal femoral nail (MPFN) was designed with the intention of enhancing stability in such fracture configurations. Methods: This study, conducted in East India between February 2023 and March 2025, utilized finite element modeling to evaluate the biomechanical performance of the MPFN compared with two widely used intramedullary implants: the Proximal Femoral Nail Antirotation (PFNA) and the InterTAN nail. An AO/OTA 31-A3.1 ROIF model was reconstructed using Mimics software. Each implant was virtually applied, and the models were subjected to axial, bending, and torsional loading. Stress distribution and displacement patterns were analyzed under physiologic load conditions. Results: The MPFN model demonstrated a more favorable stress distribution than PFNA and InterTAN under an axial load of 2,100 N. Bone stresses were significantly lower in the MPFN construct compared to the other two systems. Displacement analysis showed a 12.6% reduction with the MPFN relative to PFNA under axial load. Similar biomechanical superiority of the MPFN was observed under bending and torsional stresses. Conclusion: Among the three fixation systems tested, the modified proximal femoral nail exhibited the most favorable biomechanical properties, followed by the InterTAN and PFNA. These findings suggest that the MPFN may provide a biomechanically reliable alternative for treating reverse obliquity intertrochanteric fractures in the East Indian population. Clinical Relevance: The superior biomechanical stability of the MPFN may translate into reduced implant failure, improved fracture healing, and better functional outcomes for patients with reverse obliquity intertrochanteric fractures.***

Keywords: reverse obliquity intertrochanteric fracture, modified proximal femoral nail, finite element analysis, biomechanics, intramedullary fixation, East India

1. Introduction

Epidemiology and Classification

Reverse obliquity intertrochanteric fractures (ROIFs), categorized as AO/OTA 31-A3.1, are a distinct subset of proximal femoral fractures. The fracture line typically extends from the proximal- medial to the distal-lateral aspect [1], distinguishing them from AO/OTA 31-A1 and A2 patterns. ROIFs account for approximately 5.3–23.5% [2,3] of all intertrochanteric fractures, making them clinically significant due to their complexity and instability [4,5].

Limitations of Current Treatment Approaches

Surgical fixation is widely recommended to minimize complications associated with prolonged immobilization. Extramedullary implants such as dynamic hip screws (DHS), sliding hip screws, and proximal femoral plates were initially used but demonstrated significant drawbacks, including extensive surgical exposure, higher blood loss, and increased complication rates [6-8]. Consequently, intramedullary implants have become the preferred option due to their mechanical advantages—short lever arm, central fixation, minimal invasiveness, and facilitation of early mobilization [9,10]. Commonly utilized devices include the Proximal Femoral Nail Antirotation (PFNA), Gamma3 nail, and InterTAN.

Despite these advantages, fixation failure in ROIFs remains common [11]. The nearly parallel orientation of neck screws with the main fracture plane predisposes the proximal fragment to downward and lateral displacement, while the distal fragment often migrates medially. These biomechanical challenges increase the risk of screw cut-out and create stress concentration at the fracture–implant junction. Attempts to mitigate these forces using cerclage cables have shown limited success, as they add operative time, soft tissue trauma, and technical complexity [12,13]. To date, no intramedullary implant has been specifically engineered to address the unique biomechanics of ROIFs.

Need for Innovation

Considering the shortcomings of currently available fixation devices, there is a clear need for an implant designed specifically for ROIFs. Such an implant should minimize stress concentration, resist fragment migration, and provide enhanced biomechanical stability to reduce failure rates.

Study Aim

To address this gap, we developed a modified proximal femoral nail (MPFN). The MPFN features a dual-screw configuration comprising a neck screw and a subtrochanteric screw, with the latter passing through the base of the neck screw and into the main nail, anchoring below the lesser trochanter. This interlocking design aims to counteract fragment sliding and distribute stress more evenly across the construct.

The present study, conducted in East India from February 2023 to March 2025, employed finite element analysis

(FEA) to compare the biomechanical properties of the MPFN with the PFNA and InterTAN nails in AO/OTA 31-A3.1 ROIF models. We hypothesized that the MPFN would provide superior biomechanical stability under axial, bending, and torsional loading conditions.

2. Materials and Methods

Study Setting and Ethical Approval

This biomechanical study was conducted in East India between February 2023 and March 2025. Ethical approval was obtained from the institutional review board, and written informed consent was obtained from all volunteers whose CT scans were included. All experimental protocols adhered to the principles of the Declaration of Helsinki and relevant institutional guidelines.

Construction of the AO/OTA 31-A3.1 ROIF Model

High-resolution CT scans of 20 intact femora were acquired in a randomized and blinded manner. Mean values of the CT data were extracted to construct a representative three-dimensional (3D) femoral model using Mimics software (Materialise, Leuven, Belgium). Surface refinement and smoothing were carried out in Studio software (3D Systems Inc., Rock Hill, SC, USA). Cortical and cancellous regions were segmented according to Hounsfield Unit (HU) thresholds, with 700 HU defined as the boundary [14,15].

To simulate an AO/OTA 31-A3.1 reverse obliquity intertrochanteric fracture, an osteotomy plane was created at 60° relative to the sagittal plane just above the lesser trochanter. This provided the baseline fracture model for further finite element analysis (FEA) [15,16].

Implant Modeling

Computer-aided design (CAD) software was used to generate 3D models of three implants: the Proximal Femoral Nail Antirotation (PFNA), InterTAN nail, and the newly designed Modified Proximal Femoral Nail (MPFN).

The MPFN was designed with the following specifications:
Main nail length: 240 mm
Proximal and distal diameters: 17 mm and 10 mm, respectively
Neck screw diameter: 10 mm
Subtrochanteric screw diameter: 5 mm
Distal locking screw diameter: 5 mm

The neck screw was positioned centrally within the femoral head and neck. The subtrochanteric screw, interlocked with both the neck screw and the main nail, was anchored below the lesser trochanter at a right angle to the neck screw. The angle between the neck screw and the main nail was set at 130°. Each implant model was virtually assembled into the fracture construct. Representative anteroposterior and lateral views of the MPFN are shown in Fig. 1A.

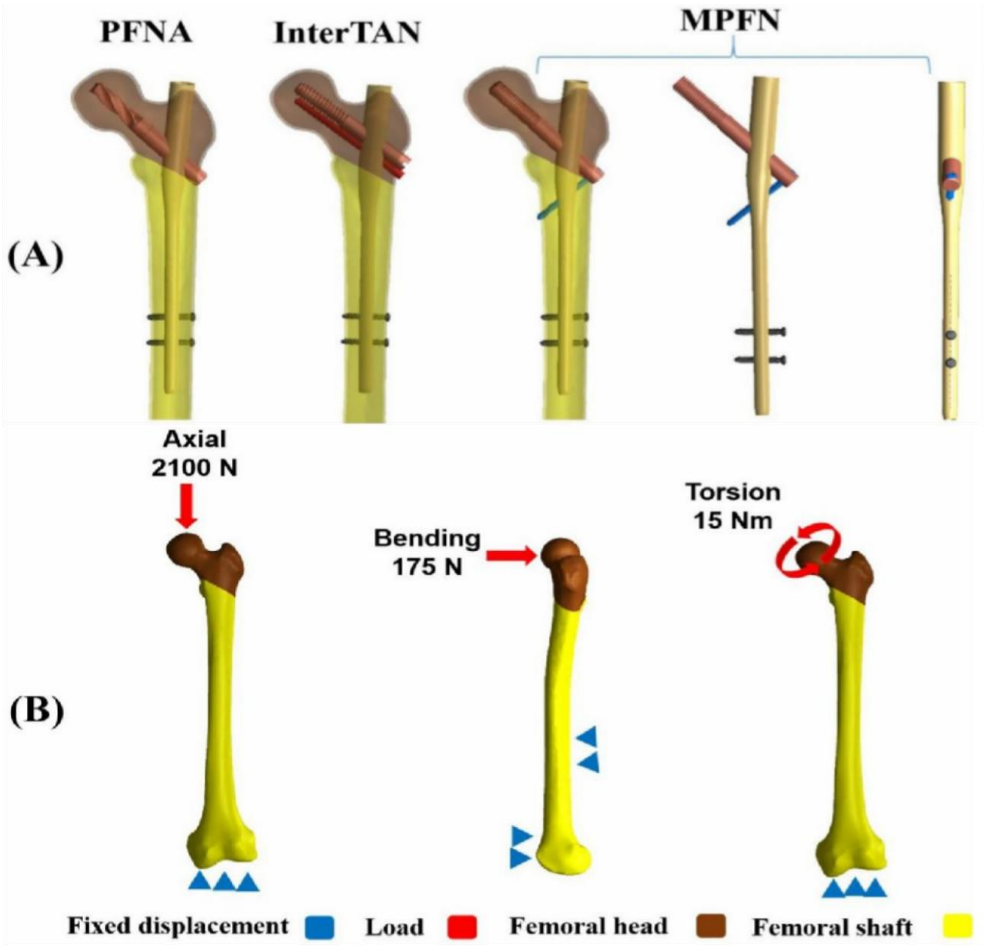

Figure 1: Schematic diagrams of the three fixation models and three boundary conditions. **(A)** Schematic diagrams of the PFNA, InterTAN, and MPFN. **(B)** Boundary conditions for axial, bending, and torsion loads. PFNA denotes the Proximal Femoral Nail Antirotation. MPFN denotes the modified proximal femoral nail

Mesh Convergence and Model Validation
Tetrahedral meshing was applied for finite element discretization. A mesh convergence study was performed using maximum von Mises stress in cortical bone as the reference variable, comparing mesh sizes of 3.0 mm, 2.5 mm, 2.0 mm, 1.5 mm, and 1.0 mm [17]. A mesh size of 1.5 mm was selected, as results at this resolution varied by less than 5% compared with 1.0 mm and 2.0 mm.

Validation was performed by applying a vertical load of 2,100 N to the intact femoral head. The computed axial stiffness was 0.52 kN/mm, which fell within the cadaveric experimental range of 0.76 ± 0.26 kN/mm, confirming reliability of the model [18].

Finite Element Settings and Boundary Conditions
Bone and implant materials were modeled as homogeneous, isotropic, and linearly elastic. Material properties were defined as follows:

Cortical bone: Young's modulus 16,800 MPa, Poisson's ratio 0.3

Cancellous bone: Young's modulus 840 MPa, Poisson's ratio 0.2

Titanium alloy (implants): Young's modulus 110,000 MPa, Poisson's ratio 0.3 [19] Element and node counts were:

PFNA model: 534,775 elements, 840,042 nodes

InterTAN model: 552,155 elements, 872,985 nodes

MPFN model: 537,984 elements, 847,212 nodes

Frictional contacts were defined between implants and bone, with a coefficient of 0.415. Loading conditions were set as follows (Fig. 1B):

Axial loading: 2,100 N vertically on the femoral head, condyles fully constrained. **Bending loading:** distal femur fixed, 175 N lateral force applied to the femoral head. **Torsional loading:** distal femur fixed, 15 Nm torque applied along the femoral neck axis.

Outcome Measures and Data Analysis
Biomechanical performance was assessed by recording:
1) Maximum von Mises stress in bone and implants.
2) Maximum displacement of the construct.
3) Displacement across the fracture surface.

The PFNA model was designated as the reference construct, given its widespread clinical use. The percent difference (PD) of parameters for the InterTAN and MPFN models relative to PFNA was calculated using the formula:

$$PD = (P_1 - P_a) / P_1 \quad X\ 100\%$$

where P1 is the value for PFNA and Pa is the value for InterTAN or MPFN.

3. Results

Maximum stress on implants under three simulated loads
The nephograms of maximum stress on implants under axial, bending, and torsional loads are shown in **Figure 2**. In the PFNA and InterTAN models, von Mises stress concentrated at the junction between the neck screw and the main nail, whereas in the MPFN model, stress localized at the junction of the subtrochanteric screw, neck screw, and main nail.

Under an axial load of 2,100 N, the maximum implant stresses were **241.34 MPa (PFNA), 259.13 MPa (InterTAN), and 214.55 MPa (MPFN)**. Corresponding values under bending load were **64.83 MPa, 58.49 MPa, and 53.98 MPa**, and under torsional load of 15 Nm were **53.53 MPa, 59.30 MPa, and 48.04 MPa**, respectively. Across all three loading conditions, the MPFN demonstrated the lowest implant stresses. Compared with the PFNA, stress reduction with MPFN was **11.1% (axial), 16.7% (bending), and 10.2% (torsion)**.

Maximum stress on bones under three simulated loads
The nephograms of maximum stress on femurs under axial, bending, and torsional loads are presented in **Figure 3**. Under axial load, the maximum bone stresses were **174.92 MPa (PFNA), 125.72 MPa (InterTAN), and 123.94 MPa (MPFN)**. For bending load, the stresses were **60.20 MPa, 56.35 MPa, and 51.04 MPa**, while under torsional load they were **61.19 MPa, 27.64 MPa, and 34.46 MPa**, respectively.

The MPFN model consistently showed lower bone stresses than PFNA and InterTAN under axial and bending loads, and lower than PFNA under torsion. Compared with PFNA, stress reduction with MPFN was **29.1% (axial), 15.2% (bending), and 43.7% (torsion)**.

Maximum displacement under three simulated loads
The nephograms of maximum displacement are displayed in **Figure 4**. Under axial loading, the maximum displacement was **19.35 mm (PFNA), 18.58 mm (InterTAN), and 16.91 mm (MPFN)**. Under bending load, the displacement values were **0.49 mm, 0.50 mm, and 0.43 mm**, and under torsional load they were **3.12 mm, 3.37 mm, and 2.55 mm**, respectively.

The MPFN consistently exhibited lower displacements than PFNA and InterTAN across all conditions. Compared with PFNA, displacement reduction with MPFN was **12.6% (axial), 10.9% (bending), and 18.1% (torsion)**.

Maximum displacement of fracture surface (MDFS) under three simulated loads
The nephograms of MDFS are shown in **Figure 5**. Under axial loading, MDFS values were **13.51 mm (PFNA), 13.82 mm (InterTAN), and 12.25 mm (MPFN)**. Under bending load, MDFS values were **0.10 mm, 0.07 mm, and 0.07 mm**, while under torsional load they were **2.15 mm, 2.32 mm, and 1.78 mm**, respectively.

The MPFN model consistently produced the lowest fracture

surface displacement across all load conditions. Compared with PFNA, MDFS reduction with MPFN was **9.3% (axial), 33.4% (bending), and 17.0% (torsion)**.

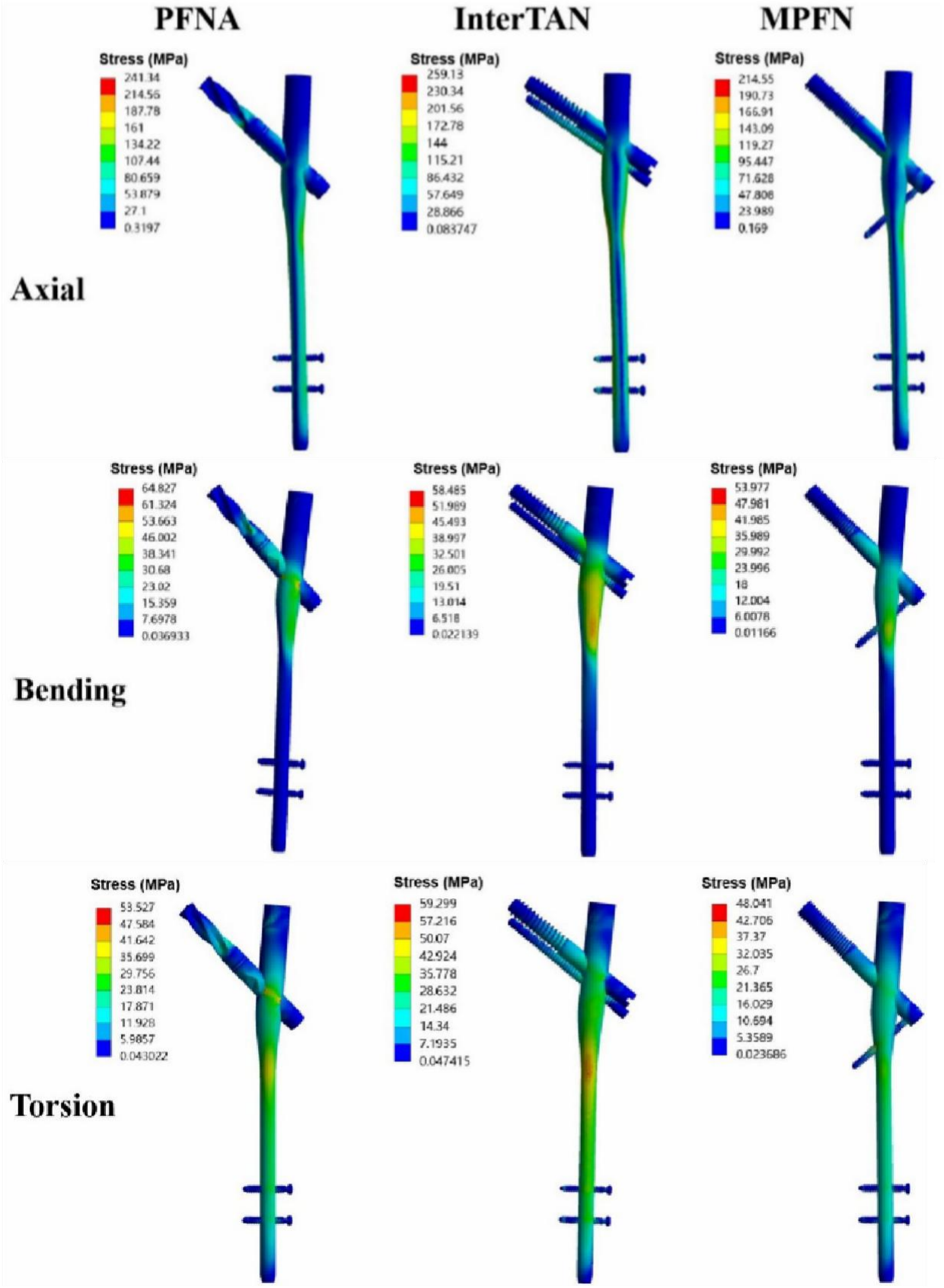

Figure 2: Maximum stress on implants for the PFNA, InterTAN, and MPFN models under axial, bending, and torsion loads. PFNA denotes the Proximal Femoral Nail Antirotation. MPFN denotes the modified proximal femoral nail.

4. Discussion

From an overall perspective, our findings demonstrate that the MPFN consistently exhibited lower maximum implant and bone stresses, as well as smaller displacements, compared with PFNA and InterTAN under axial, bending, and torsional loading conditions.

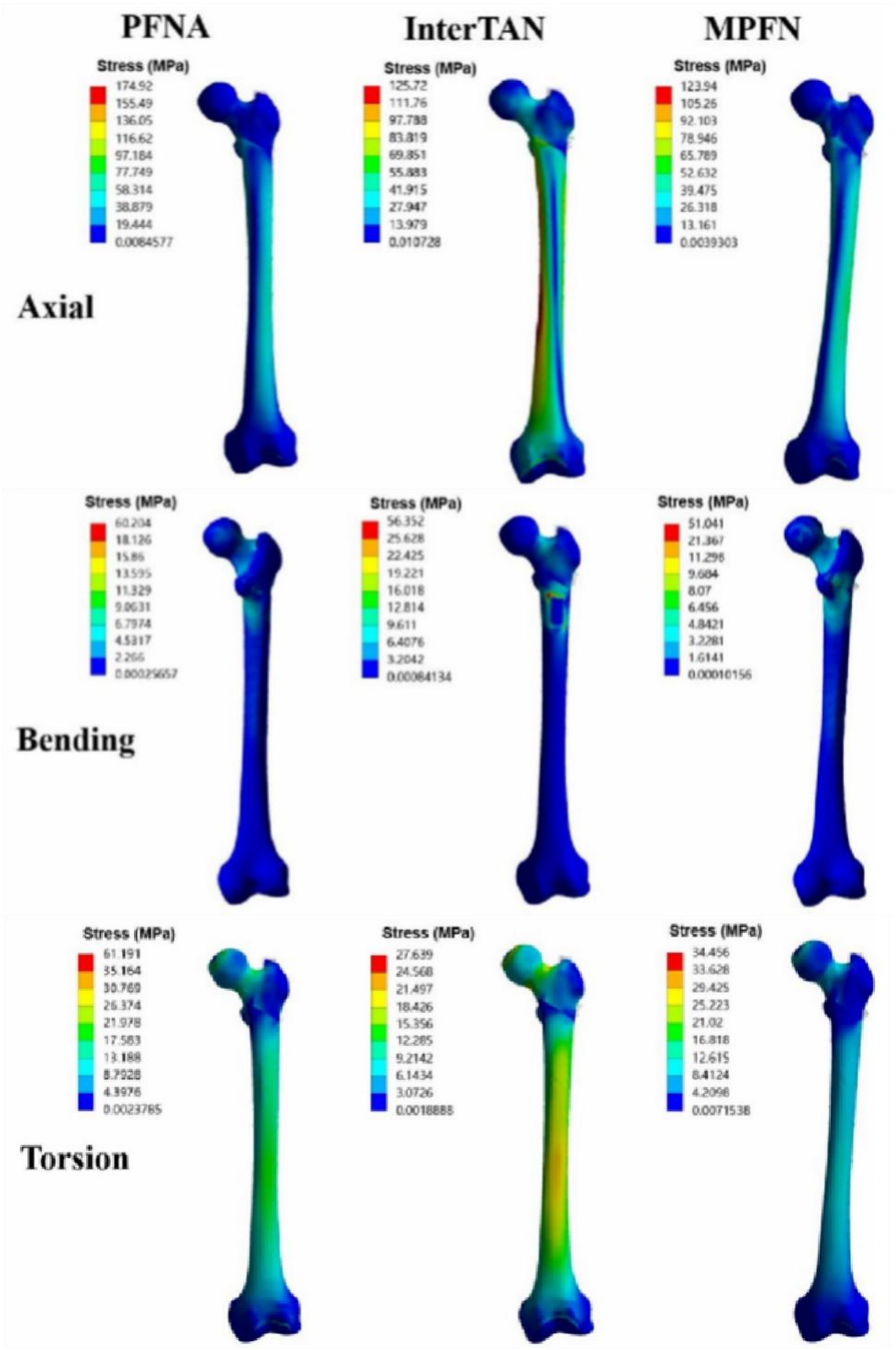

Figure 3: Maximum stress on bones for the PFNA, InterTAN, and MPFN models under axial, bending, and torsion loads. PFNA denotes the Proximal Femoral Nail Antirotation. MPFN denotes the modified proximal femoral nail.

These results indicate that the MPFN offers superior biomechanical performance and may represent an advantageous strategy for the treatment of reverse obliquity intertrochanteric fractures (ROIFs).

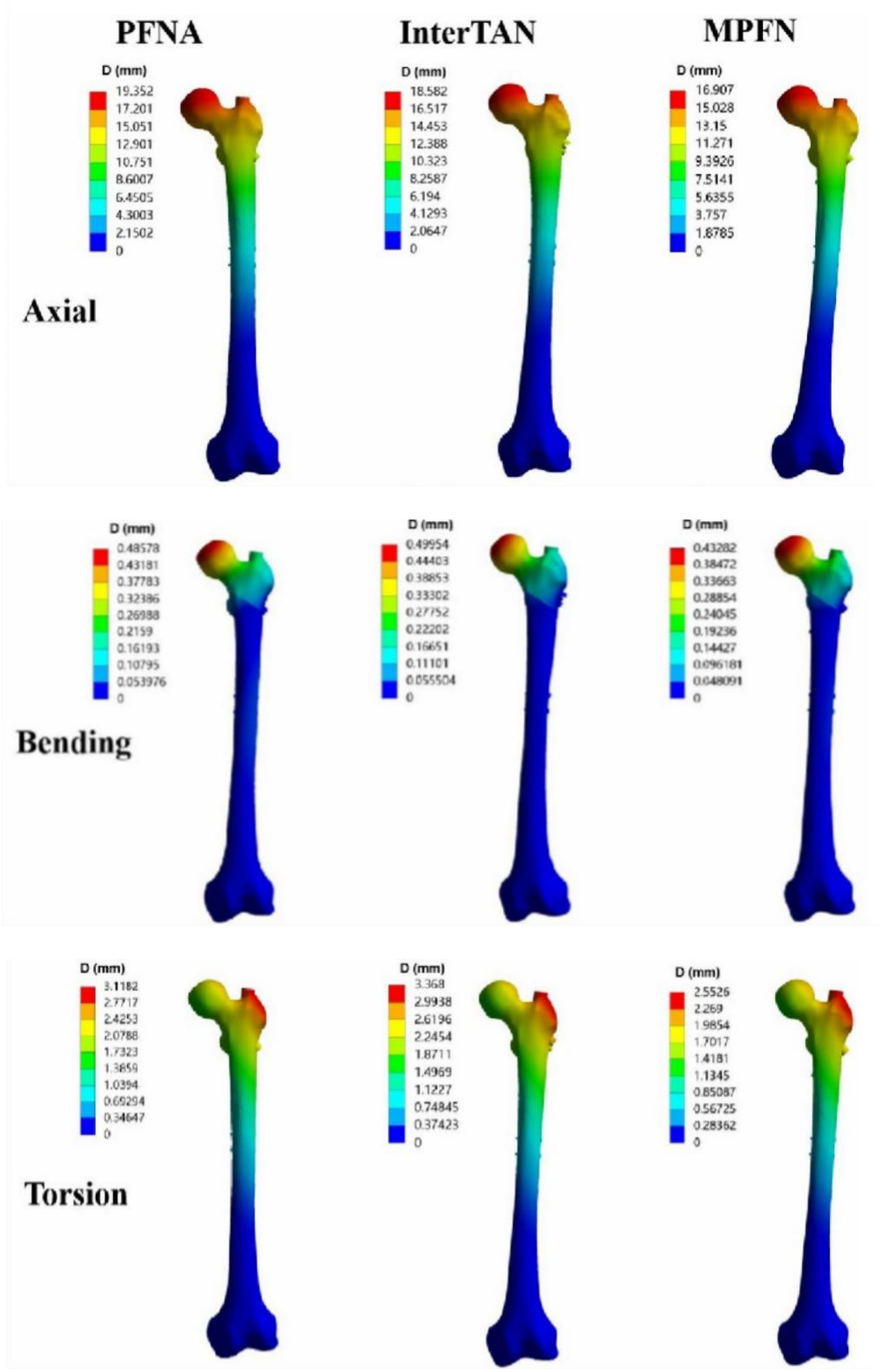

Figure 4: Maximum displacement for the PFNA, InterTAN, and MPFN models under axial, bending, and torsion loads. PFNA denotes the Proximal Femoral Nail Antirotation. MPFN denotes the modified proximal femoral nail.

Intramedullary fixation remains the most widely recommended method for managing unstable trochanteric fractures, including ROIFs [20,21]. This central fixation technique allows early partial or full weight-bearing, thereby reducing bed-rest–related complications [22].

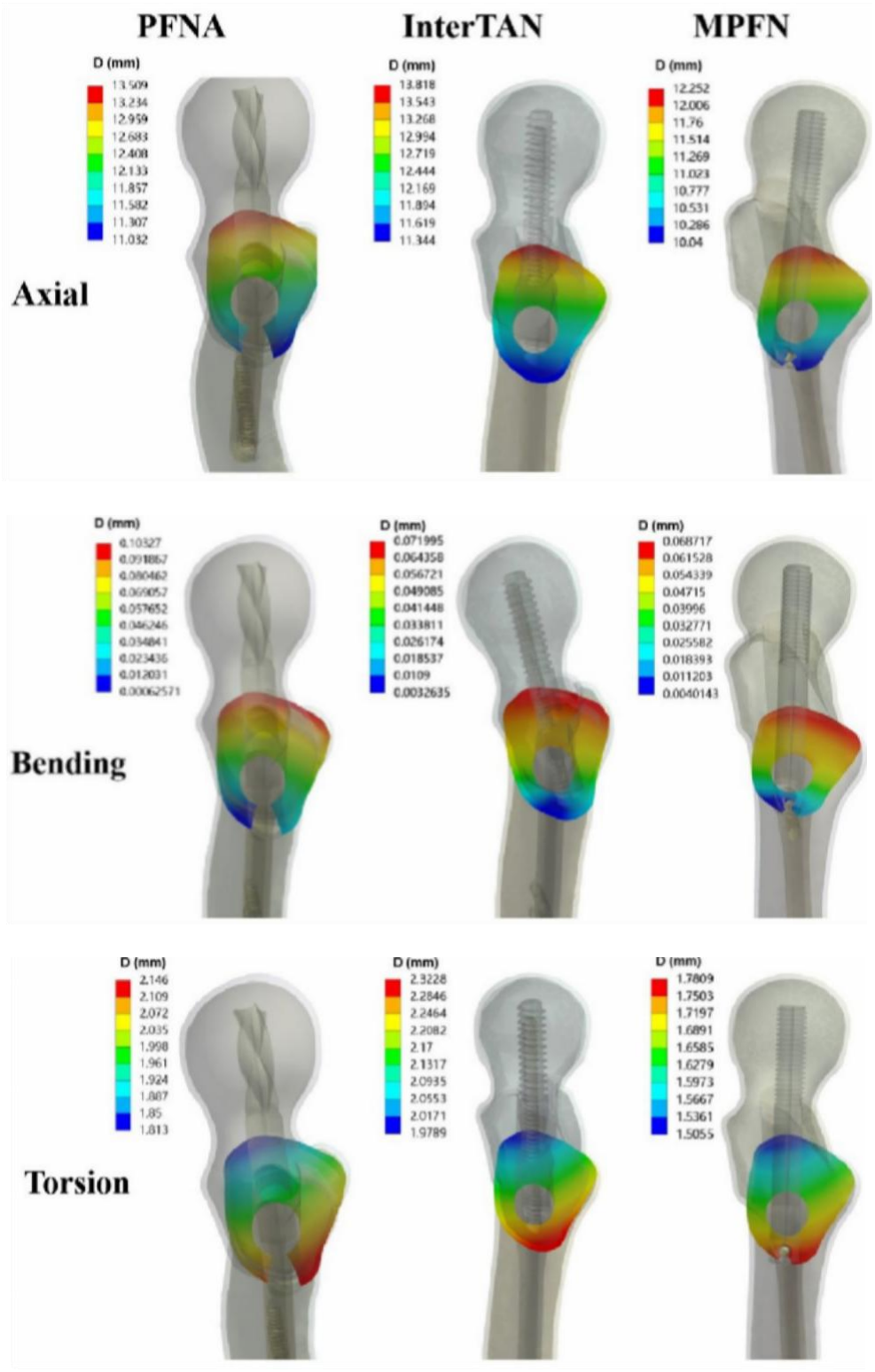

Figure 5: Maximum displacement of fracture surface for the PFNA, InterTAN, and MPFN models under axial, bending, and torsion loads. PFNA denotes the Proximal Femoral Nail Antirotation. MPFN denotes the modified proximal femoral nail.

Previous studies have shown that stresses on the femoral head surface can reach two to three times body weight during walking [23], supporting our use of a 2,100 N axial load in finite element simulations. The MPFN's unique design likely contributes to its superior axial stiffness. Specifically, the interlocking configuration of the neck screw and subtrochanteric screw restricts proximal fragment sliding, while the subtrochanteric screw helps disperse stress at the junction of the main nail and neck screw. These factors reduce the risk of implant failure compared with PFNA and InterTAN.

Antirotational stability is a critical determinant of fixation success in ROIFs, yet it has been less frequently addressed in the literature. In our study, the MPFN demonstrated enhanced antirotation compared with PFNA and InterTAN. This advantage can be explained by its structural configuration: a small rigid triangular construct is formed between the main nail, neck screw, and subtrochanteric screw, while a larger triangular structure is created between the neck screw, subtrochanteric screw, and medial wall of the proximal femur. This conforms to Zhang et al.'s principle of triangular stability [24].

The Proximal Femur Bionic Nail (PFBN), designed based on this principle, has demonstrated superior fixation of AO/OTA 31-A1.3 and A3 fractures compared with PFNA and InterTAN [25,26]. However, PFBN relies on two neck screws positioned above the main fracture line, which may not provide sufficient antirotation in ROIFs. In contrast, the MPFN places its neck screw and subtrochanteric screw on opposite sides of the fracture line, locked at a right angle, thereby enhancing rotational, compressive, and bending resistance.

Medial support has also been highlighted as a key factor for intertrochanteric fracture stability [27–29]. Chen et al. reported that loss of reduction due to medial wall comminution occurred in ~20% of patients [27], while Song et al. identified medial wall comminution as a predictor of implant failure after intramedullary fixation [29]. Nie et al. further demonstrated biomechanically that the medial wall is more critical than the lateral wall in maintaining fracture stability [28]. Based on this concept, the Medial Support Nail-II (MSN-II) was developed, incorporating triangular stability for ROIF fixation. Nie et al. showed that MSN-II provided greater stability than PFNA-II under increasing axial loads [16]. However, because its neck screws are almost parallel to the fracture line, its anti-sliding effect is limited. By contrast, the MPFN leverages its subtrochanteric screw, oriented at a right angle to the neck screw, to provide both medial support and strong anti-sliding resistance.

5. Limitations

This study has several limitations. First, finite element modeling did not account for muscles, ligaments, or tendons, a limitation common to similar biomechanical evaluations of novel implants [17,30]. However, our primary objective was to assess implant–bone interactions, making this simplification acceptable. Second, loading conditions were simplified to axial compression, bending, and torsion, whereas physiological loading during gait is more complex. Future studies will incorporate dynamic loading patterns reflective of daily activities. Third, the femur was modeled as a homogeneous material, while actual bone exhibits heterogeneous properties. Current digital simulation techniques are not yet able to fully replicate this heterogeneity. Finally, further cadaveric and clinical studies are needed to validate the biomechanical advantages of the MPFN demonstrated in our finite element analysis.

6. Conclusion

This finite element analysis demonstrated that the Medial Proximal Femoral Nail (MPFN) provides superior biomechanical stability compared with the Proximal Femoral Nail Antirotation (PFNA) and InterTAN in the fixation of reverse obliquity intertrochanteric fractures (ROIFs). The MPFN consistently showed reduced implant and bone stresses, smaller overall displacement, and decreased fracture surface motion under axial, bending, and torsional loads. These findings can be attributed to its unique design, particularly the interlocking configuration between the neck and subtrochanteric screws, which offers enhanced resistance to sliding, bending, and rotational forces while ensuring better medial support.

Although the results support the use of MPFN as a promising fixation strategy for ROIFs, further cadaveric biomechanical experiments and prospective clinical studies in East Indian populations are necessary to confirm its long-term efficacy and clinical applicability.

References

[1] Haidukewych, G. J., Israel, T. A. & Berry, D. J. Reverse obliquity fractures of the intertrochanteric region of the femur. J. Bone Joint Surg. Am. 83, 643–650 (2001).
[2] Makki, D., Matar, H. E., Jacob, N., Lipscombe, S. & Gudena, R. Comparison of the reconstruction trochanteric antigrade nail (TAN) with the proximal femoral nail antirotation (PFNA) in the management of reverse oblique intertrochanteric hip fractures. Injury 46, 2389–2393 (2015).
[3] Park, S. Y., Yang, K. H., Yoo, J. H., Yoon, H. K. & Park, H. W. The treatment of reverse obliquity intertrochanteric fractures with the intramedullary hip nail. J. Trauma. 65, 852–857 (2008).
[4] de Bruijn, K., den Hartog, D., Tuinebreijer, W. & Roukema, G. Reliability of predictors for screw cutout in intertrochanteric hip fractures. J. Bone Joint Surg. Am. 94, 1266–1272 (2012).
[5] Hsueh, K. K. et al. Risk factors in cutout of sliding hip screw in intertrochanteric fractures: an evaluation of 937 patients. Int. Orthop. 34, 1273–1276 (2010).
[6] Larsson, S., Friberg, S. & Hansson, L. I. Trochanteric fractures. Mobility, complications, and mortality in 607 cases treated with the sliding-screw technique. Clin. Orthop. Relat. Res. 260, 232–241 (1990).
[7] Nuber, S., Schönweiss, T. & Rüter, A. Stabilisation of unstable trochanteric femoral fractures. Dynamic hip screw (DHS) with trochanteric stabilisation plate vs.

proximal femur nail (PFN). Unfallchirurg 106 (1), 39–47 (2003).
[8] Zha, G. C., Chen, Z. L., Qi, X. B. & Sun, J. Y. Treatment of pertrochanteric fractures with a proximal femur locking compression plate. Injury 42 (11), 1294–1299 (2011).
[9] Lu, G. L., Li, S. J. & Li, W. X. Biomechanical study of extramedullary and intramedullary fixation in the treatment of unstable intertrochanteric reversed-tilt fractures of the femur. Ann. Transl Med. 10(4), (2022).
[10] Şensöz, E., Ergun, S., Kayaalp, M. E. & Eceviz, E. The comparison of dynamic condylar screw plate to proximal femoral nail in reverse oblique and transverse intertrochanteric fractures: a retrospective study on 61 patients. Cureus 15(3), (2023).
[11] Chou, D. T., Taylor, A. M., Boulton, C. & Moran, C. G. Reverse oblique intertrochanteric femoral fractures treated with the intramedullary hip screw (IMHS). Injury 43(6), (2012).
[12] Afsari, A. et al. Clamp-assisted reduction of high subtrochanteric fractures of the femur. J. Bone Joint Surg. Am. 91, 1913–1918 (2009).
[13] Robinson, C. M., Houshian, S. & Khan, L. A. Trochanteric-entry long cephalomedullary nailing of subtrochanteric fractures caused by low energy trauma. J. Bone Joint Surg. Am. 87, 2217–2226 (2005).
[14] Bai, H. et al. Biomechanical evaluation of three implants for treating unstable femoral intertrochanteric fractures: finite element analysis in axial, bending and torsion loads. Front. Bioeng. Biotechnol. 11, 1279067 (2023).
[15] Eberle, S., Gerber, C., Von Oldenburg, G., Hogle, F. & Augat, P. A biomechanical evaluation of orthopaedic implants for hip fractures by finite element analysis and in-vitro tests. Proc. Inst. Mech. Eng. H. 224, 1141–1152 (2010).
[16] Nie, S. B. et al. Medial support nail and proximal femoral nail antirotation in the treatment of reverse obliquity inter-trochanteric fractures (Arbeitsgemeinschaft fur Osteosynthesfrogen/Orthopedic Trauma Association 31-A3.1): a finite-element analysis. Chin. Med. J. (Engl) 133(22), (2020).
[17] Ding, K. et al. Proximal femoral bionic nail-a novel internal fixation system for the treatment of femoral neck fractures: a finite element analysis. Front. Bioeng. Biotechnol. 11, (2023).
[18] Papini, M., Zdero, R., Schemitsch, E. H. & Zalzal, P. The biomechanics of human femurs in axial and torsional loading: comparison of finite element analysis, human cadaveric femurs, and synthetic femurs. J. Biomech. Eng. 129 (1), 12–19 (2007).
[19] Li, J., Zhao, X., Hu, X., Tao, C. & Ji, R. A theoretical analysis and finite element simulation of fixator-bone system stiffness on healing progression. J. Appl. Biomater. Funct. Mater. 16, 115–125 (2018).
[20] Meinberg, E. G., Agel, J., Roberts, C. S., Karam, M. D. & Kellam, J. F. Fracture and dislocation classification compendium-2018. J. Orthop. Trauma. 32, S1–S10 (2018).
[21] D'Arrigo, C. et al. Intertrochanteric fractures: comparison between two different locking nails. Int. Orthop. 36, 2545–2551 (2012).
[22] Zehir, S., Zehir, R., Zehir, S., Azboy, I. & Haykir, N. Proximal femoral nail antirotation against dynamic hip screw for unstable trochanteric fractures; a prospective randomized comparison. Eur. J. Trauma. Emerg. Surg. 41, 393–400 (2015).
[23] Bergmann, G. et al. Hip contact forces and gait patterns from routine activities. J. Biomech. 34, 859–871 (2001).
[24] Zhang, Y., Chen, W. & Zhang, Q. A triangular-supported intramedullary nail for femoral neck and intertrochanteric fractures. Patent CN201524132U, (2010).
[25] Wang, Y. et al. Finite element analysis of proximal femur bionic nail (PFBN) compared with proximal femoral nail antirotation and InterTan in treatment of intertrochanteric fractures. Orthop. Surg. 14(9), (2022).
[26] Yang, Y. J. et al. Comparative study of a novel proximal femoral bionic nail and three conventional cephalomedullary nails for reverse obliquity intertrochanteric fractures: a finite element analysis. Front. Bioeng. Biotechnol. 12 (0), 1393154 (2024).
[27] Chen, S. Y. et al. A new fluoroscopic view for evaluation of anteromedial cortex reduction quality during cephalomedullary nailing for intertrochanteric femur fractures: the 30 oblique tangential projection. BMC Musculoskelet. Disord. 21 (1), 719 (2020).
[28] Nie, B., Chen, X., Li, J., Wu, D. & Liu, Q. The medial femoral wall can play a more important role in unstable intertrochanteric fractures compared with lateral femoral wall: a biomechanical study. J. Orthop. Surg. Res. 12, 197 (2017).
[29] Song, H., Chang, S. M., Hu, S. J., Du, S. C. & Xiong, W. F. Calcar fracture gapping: a reliable predictor of anteromedial cortical support failure after cephalomedullary nailing for pertrochanteric femur fractures. BMC Musculoskelet. Disord. 23 (1), 175 (2022).
[30] Ren, W. et al. The study of biomechanics and clinical anatomy on a novel plate designed for posterolateral tibial plateau fractures anterolateral approach. Front. Bioeng. Biotechnol. 10, (2022).